coatings

MDPI

Article

Biodegradable Optical Fiber in a Soft Optoelectronic Device for Wireless Optogenetic Applications

Sungkeun Han and Gunchul Shin *

School of Materials Science and Engineering, University of Ulsan, 12 Technosaneop-ro 55 beon-gil, Nam-gu, Ulsan 44776, Korea; gun412@naver.com

* Correspondence: gunchul@ulsan.ac.kr; Tel.: +82-52-712-8067

Received: 15 October 2020; Accepted: 25 November 2020; Published: 26 November 2020

Abstract: Optogenetics is a new neuroscience technology that uses light-responsive proteins to stimulate neurons with light and control the emotions and/or behavior of animals. There are a few approaches to deliver light to neurons in vivo, including a using an optical fiber that can send light from an external source to a target neuron, directly inserting a light-emitting device, and shooting light to penetrate tissue from the outside. Among these methods, inserting a wireless light-emitting device that is capable of being used for an experiment while leaving an animal completely free is a method that has been studied in recent years. At the same time, the possibility of causing mechanical and thermal damage to neural tissues has been highlighted as an issue due to the stiffness of robust injection tools and the photoelectric efficiency of light-emitting diodes (LEDs). In this study, we developed a device that can send light from a wireless light-emitting device to a target neuron without mechanical and thermal effects and analyzed the optical and thermal characteristics of the device to be used for optogenetic studies.

Keywords: optogenetic; optoelectronic; biodegradable; optical fiber; waveguide; wireless; LED

1. Introduction

The brain receives and analyzes electrical signals from various nerves and, in response, releases hormones to manage emotions and stimulate motor nerves to control behavior. In other words, neuronal stimulation is a basic means to control the systems of the living body. Research has long been underway on methods of stimulating the neurons of the brain, the most common of which is to inject a metal probe or arrays of probes into the brain and then stimulate neurons with electricity from the tip of the probe [1–3]. This is a simple and relatively easy-to-operate device, but since most biological tissue conducts electricity the problem arises that it is almost impossible to finely control a specific neuron. Optogenetics have been studied with a technique that enables the single-neuron stimulation of genetically modified neurons to generate currents in response to light, whereas nearby neurons that are not light-sensitive are not stimulated by light [4,5]. In addition to biological modification, there remains the problem of technically delivering light to a target neuron, which is solved by using laser equipment as a light source and an optical fiber as a waveguide that can reflect light inside the fiber [6–8]. Lasers and optical fibers have been used for optogenetic studies for many years, but an issue that has recently been recognized is that actual animal behavior control experiments can be influenced because the animals are tethered to optical fibers. Thus, instead of using a wired optical fiber system, many studies have been conducted by attaching or inserting a light-emitting device that is operated wirelessly [9–18].

Micro light-emitting diodes (LEDs), as light-emitting sources installed in micro needles which are wirelessly driven, have been reported with reliable behavioral data [9]. This was the first study to use a wireless power system and micro-LED device for studying animal behavior without a wired

connection between the animal and the surroundings. After that, a small, lightweight, flexible, and stretchable form that allowed the wireless stimulation of neurons with freely moving animals was reported [10,11]. Wireless optogenetic systems are expanded to the control of behavior by integrating systems that stimulate the nervous system and deliver drugs wirelessly at the same time [14]. To date, various optogenetic technologies in wireless form have been developed. However, the issues which originated from heat generation occur due to the photoelectric efficiency problem of the optoelectronic device converting electricity to light [9,11,15,17]. Due to the possibility of thermal damage to biological tissues, the limitation of the light intensity and heat dissipation systems of devices is a problem that remains to be solved. In addition, due to the tissue damage that arises from robust injection tools, there is a limitation regarding the selection of materials and/or devices that can be used for optogenetic implantation [9,11–13]. In this paper, we developed a new type of optogenetic device using a biodegradable shell on a soft optical fiber that transmits light from a wireless light-emitting device to a target neuron without further mechanical and thermal damage and analyzed this system optically, mechanically, and thermally. Near-field power transfer-based wireless approaches can also help to expand the possibilities to apply this device and system to various circumstances without direct connection and mobile healthcare area as well. Various previously reported wireless optogenetic devices are listed in Table 1 for a comparison of their properties with those of the device we report here.

Table 1. Comparison of various wireless optogenetic devices.

Property/Device	This Work	Kim et al., Science 2013 [9]	Park et al., Nat. Biotech. 2015 [11]	Montgomery et al., Nat. Methods 2015 [10]	Shin et al., Neuron 2017 [15]	Emara et al., IEEE Trans. Biomed. Eng. 2019 [19]	Mickle et al., Nature 2019 [17]
Size of device (mm^3)	18 × 18 × 1	~20 × 15 × 15	0.7 × 3.8 × 6	2 × 2 × 2	9.8 × 9.8 × 1.3	15 × 13 × 15	~30 × 30 × 1
Dimension of injection part	Diameter(D): 384 μm, (during injection) D: 254 μm (after injection)	~400 μm × 100 μm (during injection), ~400 μm × 10 μm (after injection)		D: ~400 μm	~350 μm × 100 μm	D: 200 μm	
Weight	0.5 g	~2.5 g	16 mg	20~40 mg	~30 mg	3.8 g	
Main application	Deep brain stimulation (DBS)	DBS	Peripheral nerve stimulation (PNS)	DBS & PNS	DBS	DBS	PNS
Wireless control	Near field communication (NFC)	Radio frequency (RF, 900 MHz)	RF (2.4 GHz)	RF with Resonant cavity	NFC	Battery/infrared	Battery/NFC/Bluetooth
Wireless range (distance from antenna)	~30 cm	~1 m	~50 cm	<10 cm	~30 cm	~60 cm	~30 cm
Fully implantable	Yes	Head-mountable	Yes	Yes	Yes	Head-mountable	Yes
Light source	Micro LED	Micro-LED	Micro-LED	Micro-LED	Micro-LED	Laser diode	Micro-LED
Position of light source	Subdermal	Deep brain	Subdermal/epidural	Deep brain/subdermal	Deep brain	Head-mount	Around bladder
Type of implanted probe	Optical fiber with a biodegradable layer	Polymer probe with a removable injection tool	Polymer probe	Rigid twisted 36 G wire	Thick Polymer probe	Optical fiber	Polymer probe
Limitation of LED operation due to thermal issue	No	Yes	Yes	Yes	Yes	No	Yes
Mechanical properties of device	Soft, flexible, low modulus, biodegradable	Flexible	Soft, flexible, stretchable	Rigid	Flexible	Rigid	Soft, flexible, stretchable
Additional function	Operable with smartphone	Integrated sensors				Tapered fiber	Operable with smartphone

2. Materials and Methods

2.1. Fabrication Procedure

Device fabrication began by attaching a 5 μm-thick aluminum foil to a thermally cured 100 μm-thick polydimethylsiloxane (PDMS) substrate. The PDMS substrate was prepared by mixing Sylgard 184 (Dow Corning, Midland, MI, USA) and a curing agent in a 10:1 mass ratio, removing bubbles and drop-casting on a slide glass for 30 min at 110 °C. The aluminum foil was cut to 3 × 3 cm and bonded onto the cured PDMS substrate. Then, micro-patterns including a receiving antenna (line width: 200 μm; line space: 250 μm, six turns, diameter: 18 mm) and an LED chip bonding area were designed using a computer-aided design (CAD, AutoCAD, Autodesk, Inc., San Rafael, CA, USA) program. The designed circuits were patterned/etched by CO_2 laser marking equipment (CO_2 laser marker, Hyosung Electronics, Bucheon, Korea), and an optical microscope (Stereomicroscope, SDPTOP, Optika, Via Rigla, Italy) and a multimeter (Fluke 87, Fluke, Everett, WA, USA) were used to identify electrically shorted or less etched areas. After removing unnecessary aluminum parts, a micro-LED (C450TR2227, Cree, Durham, NC, USA) was soldered using soldering paste (SMD290SNL250T5, Chip Quik, Ancaster, ON, USA). Soldering paste was placed on the aluminum electrode pattern to which the LED was connected in a portion of about 100 μm diameter using a pointed probe. After that, the micro-LED was placed in the relevant position and connected electrically using a soldering gun (FX-951, Hakco, Osaka, Japan) with an ultra-sharp micro tip (T12-J02, Hakco, Osaka, Japan). Details of the fabrication procedure are described in a previous report [20].

2.2. Biodegradable Optical Fiber

For the optical fiber with a biodegradable shell, the PDMS solution was inserted into a Teflon tube (PTFE-32-25, SAI, Lake Villa, IL, USA) with an inner diameter (I.D.) of 254 μm. After thermal curing for 3 h at 90 °C, the Teflon tube was carefully removed. The cured PDMS tube was inserted into the center of a second Teflon tube (PTFE-28-25, SAI, Lake Villa, IL, USA) with an I.D. of 380 μm. Thermally melted Poly(Lactide-co-Glycolide) (PLGA, Merck, St. Louis, MO, USA) was added between the PDMS tube and the Teflon tube. After cooling down to room temperature, the Teflon tube was carefully removed as well. Connecting to the optoelectronic device, an optical fiber was placed exactly onto the soldered LED chip and bonded using a drop of PDMS solution using an optical microscope, followed by thermal curing. A highly reflective metal film (Pt or Au, 20 nm) was coated at the beginning of the fiber to prevent light loss. A schematic illustration of the completed optogenetic device with the optical fiber is shown in Figure 1, and the details of the fabrication procedure of the optical fiber with a biodegradable shell are presented in Figure A1.

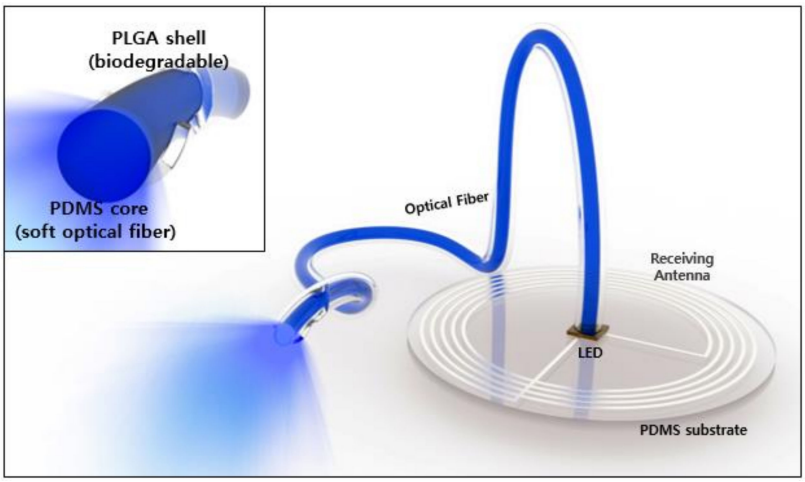

Figure 1. Schematic illustration of the soft, wireless optoelectronic device with a biodegradable Poly(Lactide-co-Glycolide)(PLGA) shell/soft Polydimethylsiloxane(PDMS) core optical fiber.

2.3. Wireless System

The coil antenna was designed to receive power using a frequency of 13.56 MHz—the radio frequency used for near-field communication (NFC). The device as operated wirelessly on top of a commercial NFC reader (ACR122, Advanced Card System, Kowloon Bay, Hong Kong), and the optical fiber (length: 50 mm) successfully delivered blue light from the micro-LED at the center of the device to a piece of paper outside of the device. Figure 2 shows a soft optoelectronic device with an optical fiber that was wirelessly operated, and a wireless power transmission system (Neurolux system, Chicago, IL, USA) capable of providing 13.56 MHz radio frequency (RF) signals at up to 10 W of RF output power. The system allowed us to manually set the antenna with the desired shape at the desired location. In this study, the transmitting antenna was constructed with a circular shape with a radius of about 20 cm and placed on top of an office desk. The inset image of Figure 2b shows that our wireless optoelectronic device works at a distance of 20 cm from the transmitting antenna. The wireless power transfer depends on the distance from the transmitting antenna horizontally and vertically as well. A modified double-loop antenna design to achieve uniformity in the performance of wireless power transfer in a 3-dimensional area ($30 \times 30 \times 12$ cm^3) has been reported before [15]. This optoelectronic device can be wirelessly operated after being implanted under the subdermal area with an optical fiber which is injected into the deep brain, as shown in the scheme of Figure 2c.

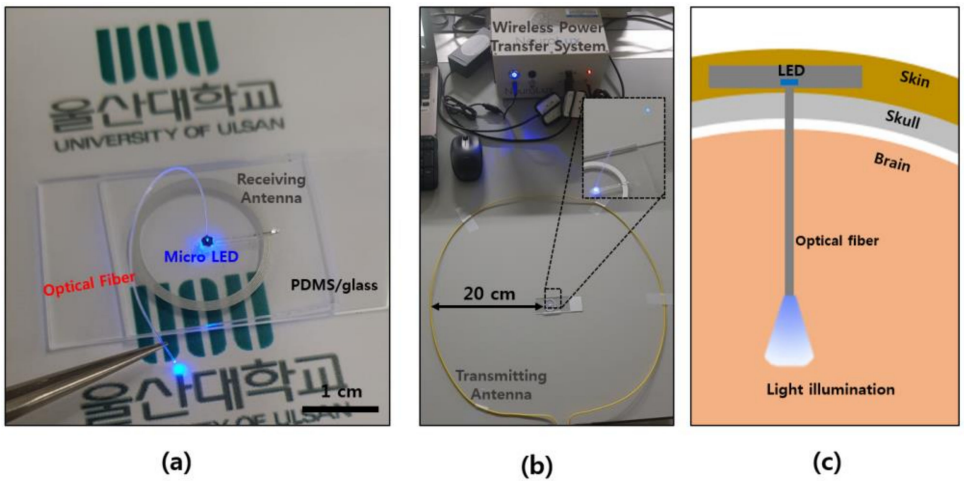

Figure 2. Optical fiber-assisted optogenetic device and wireless power transfer system. (**a**) Wirelessly operated optogenetic device with optical fiber. (**b**) Antenna set-up for wireless power transfer. (**c**) Scheme for implanted device in the deep brain.

2.4. Optical, Biodegradable, and Thermal Characterization

A spectrometer (HR4000, Ocean Optics, Largo, FL, USA) and integrating sphere were used to confirm the optical characteristics, and the light emission spectrum and optical output density of the LED were measured and calculated. An optical fiber was immersed into a phosphate buffer solution (PBS, 1 M, pH 7.4) to confirm the biodegradable properties. To analyze the thermal characteristics, an ultrathin thermal sensor and an IR camera (FLIRONE PRO, FLIR, Wilsonville, OR, USA) were used. The thermal sensor was fabricated by depositing Pt and Au on a polyethylene terephthalate (PET) film with a thickness of 5 μm, and the change in resistance was measured according to the change in the temperature of an interdigit-type Pt micro pattern.

3. Results and Discussion

3.1. Optical Characterization

3.1.1. Optical Properties of LED

Figure 3 summarizes the optical characteristics of the wireless optogenetic device with the optical fiber. The current–voltage response (Figure 3a) shows the diode characteristics of the LED chip used here, where the LED has dimensions of 220 μm (width) × 270 μm (length) × 50 μm (thickness), the junction area is 190 × 230 μm, and the forward voltage is about 3.15 V. The dominant peak of the wavelength of the LED used is 450 nm, which matches the activation peak of Channelrhodopsin-2 (ChR2), one of the light-sensitive proteins widely used in optogenetic studies. Other LEDs which have different wavelengths can also be used for different opsins as well [15]. In Figure 3b, the optical power density of the light emitted according to the current flowing through the fabricated device is shown, and the ultra-small LED chip was used to confirm the high optical density (several tens of mW/mm^2) at a low driving current (a few mA). It is thus suitable for use in optogenetic technology that can stimulate a single cell with light, and it is expected to be extended to an LED array when targeting neurons in a large area [4,5,9].

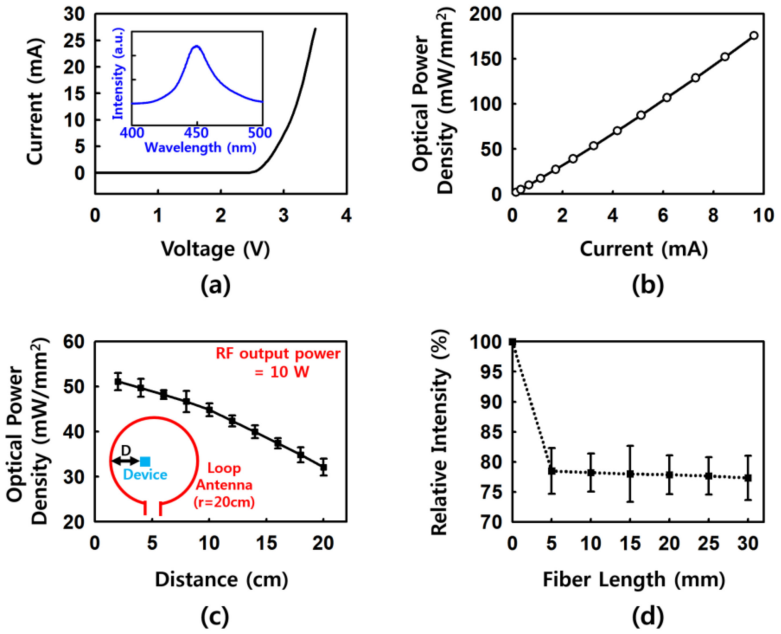

Figure 3. Optical properties of the LED and wireless optoelectronic device. (**a**) Current–voltage characteristics and emission spectra. (**b**) Current–light output characteristics. (**c**) Optical power density as a function of distance between the loop antenna and the device. (**d**) Relative intensity as a function of fiber and fiber length.

3.1.2. Wireless Operation

The optical characteristics of the wirelessly driven device are shown in Figure 3c. A transmitting antenna with a radius of 20 cm was constructed, the output power was set to 10 W in the RF generating system, and the optical density of the emitting device was measured according to the distance from the antenna. It exceeded the maximum value of 10 mW/mm^2, which is the general requirement for optogenetic stimulations [5,8,9,14,15]. Therefore, it is expected that animal experiments can be conducted by lowering the RF output power from 10 W in the desired experimental apparatuses. In addition, by configuring this in the form of a double-loop antenna instead of the single-loop antenna used in this experiment, the wireless experimental space is controlled in the three-dimensional direction [15]. The relative intensities of optical power densities according to the presence and length

of optical fibers connected to the LED chip are shown in Figure 3d. An optical power loss of about 1.1 dB occurred, which is not dB loss due to the fiber length but rather attenuation due to the lack of light reflection between the LED and the optical fiber. If a proper connector is developed, it is expected to reduce the loss budget. In the case of the currently manufactured device, the intensity value of about 77% exceeds the optogenetic requirements of 10 mW/mm^2 in the entire antenna area.

3.2. Biodegradable Properties

The optogenetic injection tool needs enough rigidity to penetrate the brain tissue without bending during injection. However, the rigid injectable tool may cause long-term mechanical damage in the soft tissue due to the modulus mismatching between them [9,11,13,14]. To relieve the mechanical issue, a rigid but biodegradable shell was added on the soft PDMS fiber. Figure 4a presents images of the optical fiber during dissolution at various times after immersion in phosphate buffer solution (PBS, 1 M, pH 7.4, Merck, St. Louis, MO, USA) at 37 °C. The PBS is a buffer saline solution which is commonly used in biological researches [21,22]. It is a water-based saline which contains NaCl, KCl, Na_2HPO_4, KH_2PO_4, etc., and maintains a constant pH of 7.4. PBS is widely used to test biodegradability, due to the fact that ion/solute concentrations of PBS are almost matched with those of the human body. The PLGA shell of an optical fiber absorbs the buffer solution and begins to dissolve, thereby leading to a reduction in its thickness and bending stiffness. The dissolution of the PLGA shell of an optical fiber in PBS at 37 °C occurs on a timescale of days. The thickness of the PLGA shell decreased as a function of time of immersion in PBS at various temperatures. The PLGA shells were completely dissolved in PBS after 6, 3, and 2 d at 37, 60, and 90 °C, respectively. Additionally, the bending stiffnesses of the optical fiber as a function of the immersion time reduced at a similar timescale to that of the decreasing thickness during the dissolution in PBS. These timescales are well matched with the timescale of recovery time, normally 3~10 days, from the optogenetic surgery of experimental animals [9,13,15]. In addition to the case of temperature of 37 °C, other data obtained at 60 and 90 °C can be also used to calculate the expected time to dissolve the biodegradable shell at different temperatures using Arrhenius scaling [15]. It would helpful to apply this device for animals which have different body temperatures and/or different biological conditions as well. In addition, the bending stiffness of around 2×10^4 N·μm^2 before degradation is enough to inject the optical fiber into optogenetical targets, such as a brain tissue [9,12,13,15]. Therefore, the biodegradable components of the optical fiber can be expected to aid in injection during surgery and to dissolve completely inside the animal body during the recovery time from the surgery. After the rigid and biodegradable PLGA shell was dissolved, soft and nonbiodegrable PDMS (Young's modulus~a few MPa) with a diameter of 254 μm remains to deliver light for optogenetic applications. Finally, a nonbiodegradable but biocompatible soft PDMS fiber with a small diameter (254 μm) will help to minimize the long-term damage to the biological tissue for optogenetic chronic studies [9,13,14].

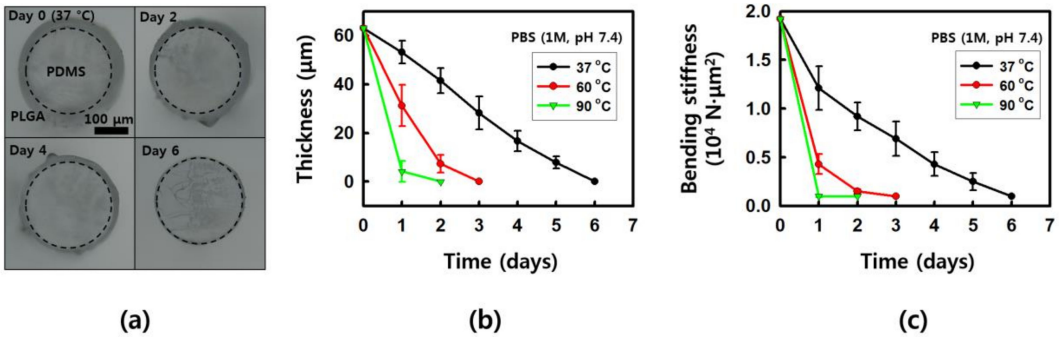

Figure 4. Biodegradable properties of the PDMS/PGLA optical fiber. (**a**) Image of a biodegradable optical fiber as a function of immersion time in phosphate buffer solution (PBS, 1 M, pH 7.4). (**b**) Results of thickness in PLGA shell as a function of the immersion time in PBS. (**c**) Results of the bending stiffness of the optical fiber as a function of the immersion time in PBS.

3.3. Theraml Characterization

3.3.1. IR Imaging

The thermal properties that can be obtained by the IR camera and micro thermal sensor probe are summarized in Figure 5. An LED is a photoelectric device that converts electricity into light and emits the remaining power as heat according to the photoelectric efficiency. This is expected to affect not only the direct insertion into the living body, but also the stimulation and the tissue damage caused by heat when the LED is placed close to the target neuron. Therefore, in the case of experiments that implant inside a brain, which is more thermally sensitive than other tissues/organs, the limit of temperature rise is considered to be within 2 °C at the maximum; even below that, the effect of heat cannot be completely excluded [9,11]. In addition, the effect is much greater in experiments using shorter wavelengths where the location of the LED is very close to the target neuron due to the wavelengths' small penetration depth through the tissue. In this study, we experimented with blue light near 450 nm that matched the activation peak of ChR2, which is known to be a light-sensitive protein. In the case of longer wavelengths—e.g., yellow, green, red, and IR—which have the same optical density, they are expected to have a relatively low thermal effect on tissues due to their longer penetration depth into the tissue [17]. Two measurement methods were used to confirm the thermal properties. First, the temperature of the LED surface and the fiber tip where light is emitted through the IR camera were checked in air (Figure 5a,b). In the case of an LED-exposed device without (WO) an optical fiber (Figure 5a), when operating at an optical density of 30 mW/mm^2, the temperature of the LED surface increased with time. After about 10 min, the temperature was confirmed to be saturated. Temperature changes of ~8.4 °C, even it does not reflect actual change of temperature of brain tissue, can be said to have a serious effect on neuronal activity [9,11]. Even if the optical density is lowered to 20 mW/mm^2, it can be confirmed as ~6.6 °C, which is not acceptable for neurological studies of the brain. In actual animal experiments, instead of continuous operation, pulses with a duty cycle of about 5% to 20% are performed to stimulate the neuron properly, which is also known to reduce heat effects [9,11,13,15]. However, depending on the animal and stimulation situation, an optical density of more than 10 mW/mm^2 and continuous operation for releasing pain may be required [17]. The required light intensity is mainly related to the sensitivity of the light-activated protein and the distance between the target neuron and the physical spot illuminated by the light—for example, the surface of an LED or the end of an optical fiber. If the surgical skill or implanting condition are not enough to place the illuminating device close to the target neuron, the actual light intensity needed to activate the optogenetic protein is higher than the required light intensity that was previously reported, due to the light absorption of tissues [23]. In this case, the effect of heat is inevitable in the case of an LED that has to be placed very close to the tissue. Therefore, to solve this problem, the optical fiber proposed in this study was introduced, and the results of the IR camera are shown in Figure 5b. Even if the LED was operated at an optical density of 20 mW/mm^2 for 10 min, the temperature at the tip of the fiber did not change by more than 0.3 °C. It was confirmed by IR imaging that the heat generated by the LED itself (temperature change of ~7 °C) could be transmitted through the optical fiber that is composed of glass and plastic, but the thermal conductivity was very low at ~0.05 W/mK, meaning that the amount of heat transferred to the actual fiber end was very limited. It was also confirmed that there was little temperature change (less than 0.3 °C) even when the optical power was raised to 30 mW/mm^2, in which case the LED showed a temperature change of ~9 °C.

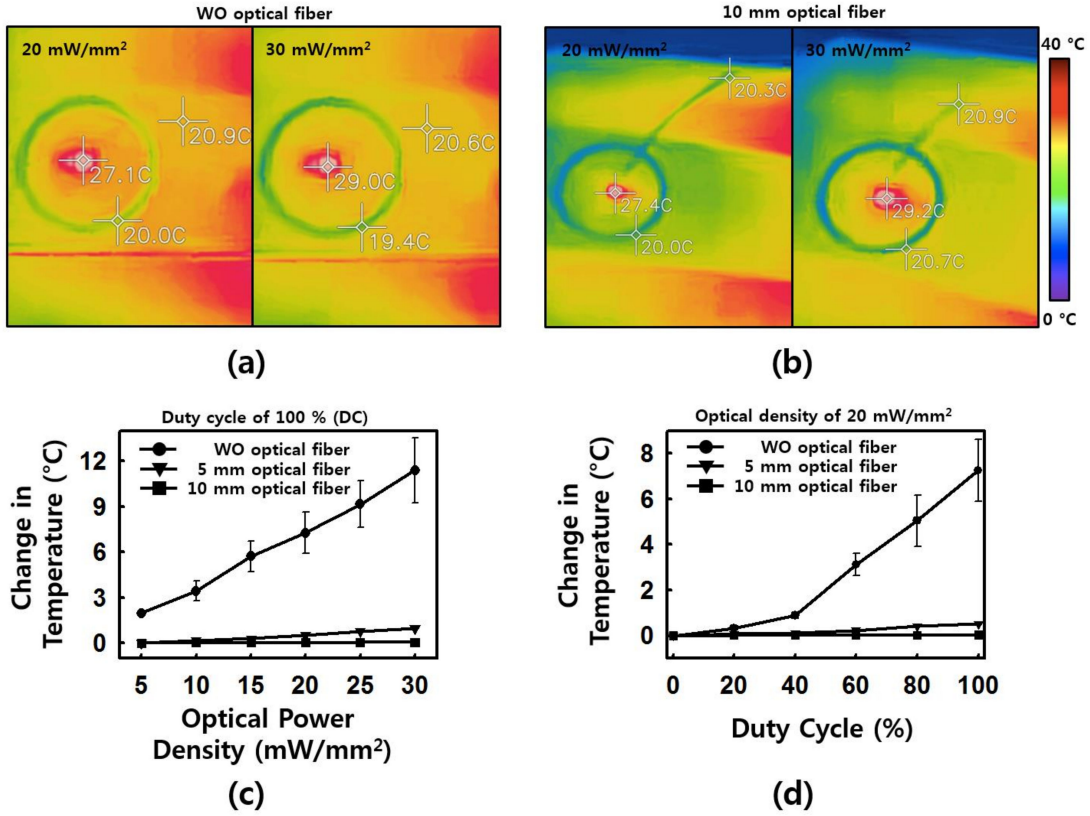

Figure 5. Thermal properties of the wirelessly operated device. (**a**) IR images of the device without and optical fiber (WO) operated at an optical power density of 20 and 30 mW/mm^2 (left and right, respectively). (**b**) IR images of the device with a 10 mm fiber operated at an optical power density of 20 and 30 mW/mm^2 (left and right, respectively). (**c**) Change in temperature as a function of optical power density for WO, 5 mm, and 10 mm fiber devices. (**d**) Change in temperature as a function of the duty cycle of pulse operation for WO, 5 mm, and 10 mm fiber devices.

3.3.2. Thermal Sensing Data

In addition to the results from the IR camera, an ultrathin thermal sensor was fabricated to check the thermal characteristics (Figure 5c,d). The interdigit-type thermal sensor composed of Pt is in contact with the LED surface or the fiber end, and the temperature change can be measured by inverting the resistance change according to the Pt temperature change. When the LED is wirelessly operated at a duty cycle of 100% (DC), the temperature change range increases according to the optical power density. In the absence of an optical fiber, the temperature change of the LED surface occurred at a maximum of 10 °C at 30 mW/mm^2. Even at 10 mW/mm^2, which is a general standard of optogenetic stimulation for ChR2 activation, there was a temperature change of ~4 °C, which can be considered to be a value that can influence brain studies. When the fiber was connected, the temperature variation range of 5 and 10 mm did not exceed 1 °C at an optical density of up to 30 mW/mm^2. If the LED was operated by a pulse, the temperature change range did not exceed 2 °C without the optical fiber within a duty cycle of about 40% at an optical density of 20 mW/mm^2, but if the duty cycle was larger than that, the temperature change increased by more than 2 °C and finally reached 7.2 °C at a 100% duty cycle. In the case of the optical fiber-connected device, there was a variation within the maximum temperature of 1 °C without a significant effect of the duty cycle.

3.4. Hydrogel and NFC Test

The above experiments, measured by an IR camera and thermal sensor, were all carried out in the atmosphere, and the temperature of the atmosphere was about 24 °C, which is not exactly the same as

that within a living animal. For example, a heat dissipation from the fiber to the biological tissue may occur during the operation of the LED after the fiber was injected. Therefore, the temperature and optical properties were confirmed within a hydrogel condition maintained at about 37 °C, similar to the heat capacity characteristics of the living body. Since the optical fiber was inserted in hydrogel, the temperature change was measured with an ultra-thin thermal sensor probe instead of IR imaging (Figure 6a). The temperature change range was maintained within 0.5 °C in an LED operated at an optical density of about 30 mW/mm^2. It is anticipated that the introduction of the optical fiber will be able to eliminate the effects of heat as much as possible, even in DC operation and high optical power operation, which was limited in previous studies. The heat dissipation effect due to heat transfer to biological tissue and biological fluid and the temperature increase effect [23] due to the heat absorbed by the tissue were not considered in this study. Further research including adjusted simulation data about the thermal effect due to surrounding tissues is needed.

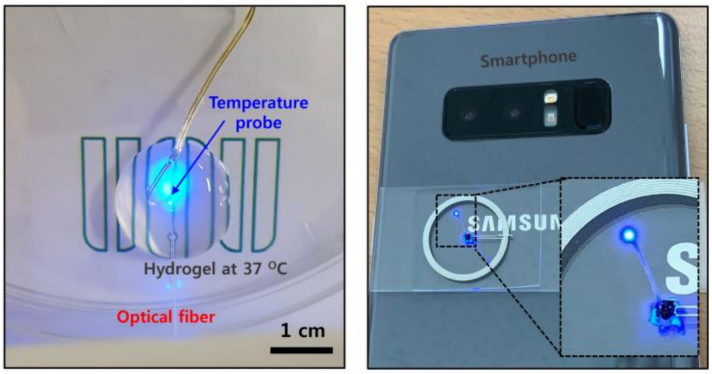

Figure 6. Wireless device operation in hydrogel and by smartphone. (**a**) Temperature measurement with an ultra-thin micro Pt probe in 37 °C hydrogel. (**b**) Wireless operation of the device powered by the near-field communication (NFC) antenna of a smartphone.

Our wireless optogenetic device uses existing NFC-based wireless communication and power transmission technology, and thus can be easily applied to commercial NFC products. As shown in Figure 6b, the wireless optogenetic device can be placed in the antenna position on the back of a commercial smartphone (in our case—Galaxy Note 8, Samsung, Suwon, Korea) when it is running in NFC mode, and the device is activated wirelessly. The phone can turn on and off the device with a simple command in the NFC setting. Without additional modification, the current NFC mode of commercial smartphone worked in very short time periods to reduce the consumption of battery at this time. Hence, if an additional commercial NFC chip is added to the device, the operation of the optogenetic device could be controlled by a mobile app on the smartphone itself. We hope that this possibility increases the device's connectivity with wireless platforms and will ultimately help achieve IoT-based personal usability for bio-medical applications.

4. Conclusions

In this study, we developed a new type of soft, wireless optogenetic device that can solve common mechanical and thermal issues of optogenetic devices by introducing an optical fiber with a biodegradable shell that delivers light indirectly instead of positioning the micro LED close to the target neuron. The results show reductions in the bending stiffness during implantation as well as reductions in the heat generated by the LED and delivered to the target while maintaining the device's optical characteristics. We expect that this device can be applied to optogenetic research that stimulates neurons by inserting it into tissues that are sensitive to heat, such as the brain, allowing behavioral and emotional animal studies to be conducted.

Author Contributions: Conceptualization, G.S.; Methodology, S.H. and G.S.; Data curation, S.H. and G.S.; Writing-original draft preparation, S.H. and G.S.; Writing-review and editing, G.S. All authors have read and agreed to the published version of the manuscript.

Funding: This work was supported by the 2017 Research Fund of the University of Ulsan.

Conflicts of Interest: The authors declare no conflict of interest.

Appendix A

Figure A1 shows the details of the procedure for fabricating a biodegradable optical fiber described here.

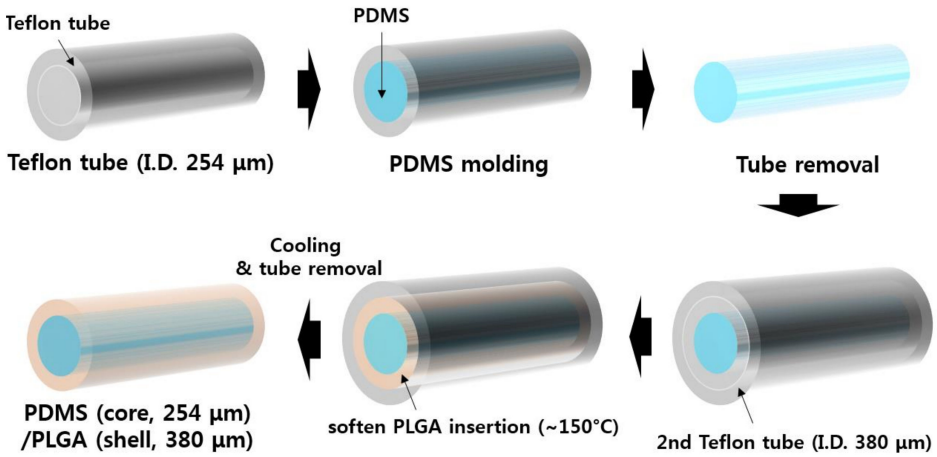

Figure A1. Schematic illustration of the fabrication procedure of an optical fiber with a biodegradable shell.

References

1. Campbell, P.K.; Jones, K.E.; Huber, R.J.; Horch, K.W.; Normann, R.A. A silicon-based, three-dimensional neural interface: Manufacturing processes for an intracortical electrode array. *IEEE Trans. Biomed. Eng.* **1991**, *38*, 758–768. [CrossRef] [PubMed]
2. Cogan, S.F. Neural stimulation and recording electrodes. *Annu. Rev. Biomed. Eng.* **2008**, *10*, 275–309. [CrossRef] [PubMed]
3. Kozai, T.D.; Langhals, N.B.; Patel, P.R.; Deng, X.; Zhang, H.; Smith, K.L.; Lahann, J.; Kotov, N.A.; Kipke, D.R. Ultrasmall implantable composite microelectrodes with bioactive surfaces for chronic neural interfaces. *Nat. Mater.* **2012**, *11*, 1065–1073. [CrossRef] [PubMed]
4. Boyden, E.S.; Zhang, F.; Bamberg, E.; Nagel, G.; Deisseroth, K. Millisecond-timescale, genetically targeted optical control of neural activity. *Nat. Neurosci.* **2005**, *8*, 1263–1268. [CrossRef] [PubMed]
5. Deisseroth, K. Optogenetics. *Nat. Methods* **2011**, *8*, 26–29. [CrossRef]
6. Fenno, L.; Yizhar, O.; Deisseroth, K. The development and application of optogenetics. *Annu. Rev. Neurosci.* **2011**, *34*, 389–412. [CrossRef]
7. Packer, A.M.; Roska, B.; Hausser, M. Targeting neurons and photons for optogenetics. *Nat. Neurosci.* **2013**, *16*, 805–815. [CrossRef]
8. Siuda, E.R.; Copits, B.A.; Schmidt, M.J.; Baird, M.A.; Al-Hasani, R.; Planer, W.J.; Funderburk, S.C.; McCall, J.G.; Gereau, R.W.; Bruchas, M.R. Spatiotemporal control of opioid signaling and behavior. *Neuron* **2015**, *86*, 923–935. [CrossRef]
9. Kim, T.I.; McCall, J.G.; Jung, Y.H.; Huang, X.; Siuda, E.R.; Li, Y.; Song, J.; Song, Y.M.; Pao, H.A.; Kim, R.-H.; et al. Injectable, cellular-scale optoelectronics with applications for wireless optogenetics. *Science* **2013**, *340*, 211–216. [CrossRef]
10. Montgomery, K.L.; Yeh, A.J.; Ho, J.S.; Tsao, V.; Mohan Iyer, S.; Grosenick, L.; Ferenczi, E.A.; Tanabe, Y.; Deisseroth, K.; Delp, S.L.; et al. Wirelessly powered, fully internal optogenetics for brain, spinal and peripheral circuits in mice. *Nat. Methods* **2015**, *12*, 969–974. [CrossRef]

11. Park, S.-I.; Brenner, D.S.; Shin, G.; Morgan, C.D.; Copits, B.A.; Chung, H.U.; Pullen, M.Y.; Noh, K.N.; Davidson, S.; Oh, S.J.; et al. Soft, stretchable, fully implantable miniaturized optoelectronic systems for wireless optogenetics. *Nat. Biotechnol.* **2015**, *33*, 1280–1286. [CrossRef] [PubMed]
12. Park, S.I.; Shin, G.; Banks, A.; McCall, J.G.; Siuda, E.R.; Schmidt, M.J.; Chung, H.U.; Noh, K.N.; Mun, J.G.; Rhodes, J.; et al. Ultraminiaturized photovoltaic and radio frequency powered optoelectronic systems for wireless optogenetics. *J. Neural Eng.* **2015**, *12*, 056002. [CrossRef] [PubMed]
13. McCall, J.G.; Kim, T.I.; Shin, G.; Huang, X.; Jung, Y.H.; Al-Hasani, R.; Omenetto, F.G.; Bruchas, M.R.; Rogers, J.A. Fabrication and application of flexible, multimodal light-emitting devices for wireless optogenetics. *Nat. Protoc.* **2013**, *8*, 2413–2428. [CrossRef]
14. Jeong, J.-W.; McCall, J.G.; Shin, G.; Zhang, Y.; Al-Hasani, R.; Kim, M.; Li, S.; Sim, J.Y.; Jang, K.-I.; Shi, Y.; et al. Wireless optofluidic systems for programmable in vivo pharmacology and optogenetics. *Cell* **2015**, *162*, 662–674. [CrossRef]
15. Shin, G.; Gomez, A.M.; Al-Hasani, R.; Jeong, Y.R.; Kim, J.; Xie, Z.; Banks, A.; Lee, S.M.; Han, S.Y.; Yoo, C.J.; et al. Flexible Near-Field Wireless Optoelectronics as Subdermal Implants for Broad Applications in Optogenetics. *Neuron* **2017**, *93*, 509–521. [CrossRef]
16. Gutruf, P.; Krishnamurthi, V.; Vazquez-Guardado, A.; Xie, Z.; Banks, A.; Su, C.-J.; Xu, Y.; Haney, C.R.; Waters, E.A.; Kandela, I.; et al. Fully Implantable Optoelectronic Systems for Battery-free, Multimodal Operation in Neuroscience Research. *Nat. Electronics* **2018**, *1*, 652–660. [CrossRef]
17. Mickle, A.D.; Won, S.M.; Noh, K.N.; Yoon, J.; Meacham, K.W.; Xue, Y.; McIlvried, L.A.; Copits, B.A.; Samineni, V.K.; Crawford, K.E. A Wireless Closed-Loop System for Optogenetic Peripheral Neuromodulation. *Nature* **2019**, *565*, 361–365. [CrossRef]
18. Edward, E.S.; Kouzani, A.Z. A Closed-Loop Optogenetic Stimulation Device. *Electronics* **2020**, *9*, 96. [CrossRef]
19. Emara, M.S.; Sileo, L.; Vittorio, M.; Pisanello, F. A wireless head-mountable device with tapered optical fiber-coupled laser diode for light delivery in deep brain regions. *IEEE Trans. Biomed. Eng.* **2019**, *66*, 1996–2009. [CrossRef]
20. Shin, G. Studies of Parylene/Silicone-Coated Soft Bio-Implantable Optoelectronic Device. *Coatings* **2020**, *10*, 404. [CrossRef]
21. Hwang, S.-W.; Tao, H.; Kim, D.-H.; Cheng, H.; Song, J.-K.; Rill, E.; Brenckle, M.A.; Panilaitis, B.; Won, S.M.; Kim, Y.-S.; et al. A Physically Transient Form of Silicon Electronics. *Science* **2012**, *337*, 1640–1644. [CrossRef] [PubMed]
22. Kang, S.-K.; Murphy, R.K.J.; Hwang, S.-W.; Lee, S.M.; Harburg, D.V.; Krueger, N.A.; Shin, J.; Gamble, P.; Cheng, H.; Yu, S.; et al. Bioresorbable Silicon Electronic Sensors for the Brain. *Nature* **2016**, *530*, 71–76. [CrossRef] [PubMed]
23. Shin, Y.; Yoo, M.; Kim, H.-S.; Nam, S.-K.; Kim, H.-I.; Lee, S.-K.; Kim, S.; Kwon, H.-S. Characterization of fiber-optic light delivery and light-induced temperature changes in a rodent brain for precise optogenetic neuromodulation. *Biomed. Opt. Express* **2016**, *7*, 4450–4471. [CrossRef] [PubMed]